energies

MDPI

Article

Optimizing the Charging Mobility of WPT-Enabled UAV to Enhance the Stability of Solar-Powered LoRaWAN IoT

Yujin Gong [1], Ikjune Yoon [2] and Dong Kun Noh [3,*]

[1] Department of Intelligent System, Soongsil University, Seoul 06978, Republic of Korea; 102177006@soongsil.ac.kr
[2] Division of AI Computer Science & Engineering, Kyonggi University, Suwon 16227, Republic of Korea; ijyoon@kyonggi.ac.kr
[3] School of AI Convergence, Soongsil University, Seoul 06978, Republic of Korea
* Correspondence: dnoh@ssu.ac.kr

Abstract: In the majority of Internet of Things (IoT) applications, persistent and stable operation is a crucial requirement. While environmental energy-harvesting technologies can enhance IoT's persistence, they do not guarantee stability. Therefore, we aim to address the stability challenges in solar-powered IoT (SP-IoT) by employing wireless power transmission (WPT) through unmanned aerial vehicles (UAVs). This study focuses on determining the optimal charging mobility of drones for WPT to enhance the stability of nodes operating in a wide area network (WAN)-based SP-IoT environment. The proposed scheme identifies nodes with insufficient solar energy harvesting and defines the optimal charging mobility parameters (hovering position, hovering time, and moving path) to efficiently transmit the drone's energy to these nodes in a balanced manner. The experimental results confirm that the proposed scheme significantly improves the stability of solar-powered IoT nodes by optimally utilizing the limited energy of the drone.

Keywords: IoT; solar-powered; LoRaWAN; wireless power transfer; stability; reliability

Citation: Gong, Y.; Yoon, I.; Noh, D.K. Optimizing the Charging Mobility of WPT-Enabled UAV to Enhance the Stability of Solar-Powered LoRaWAN IoT. *Energies* **2024**, *17*, 1617. https://doi.org/10.3390/en17071617

Academic Editor: Fengshou Gu

Received: 13 February 2024
Revised: 11 March 2024
Accepted: 25 March 2024
Published: 28 March 2024

1. Introduction

Battery-based Internet of Things (IoT) nodes suffer from longevity problems due to the limited battery capacity. There have been many studies aimed at efficiently utilizing the limited energy of batteries. Low-power wireless communication technologies such as long-range wide area networks (LoRaWANs) are one solution [1,2]. Although they improve the energy efficiency to a certain extent, this approach cannot offer a fundamental solution to the battery energy constraint problem. The problem of limited battery capacity can only be addressed by enabling nodes to generate their own energy.

To address this issue and enable the persistent operation of IoT nodes, energy-harvesting IoT nodes using environmental energy are being researched [3,4]. Environmental energy can be harvested from natural processes such as wind, heat, gravity, pressure, and the sun, or harvested from organic components in surface water and soil water using bio-fuel cells. Among them, solar energy is considered the preferable source of environmental energy for the persistent operation of IoT nodes due to the high energy density, periodic charging, and greater predictability of the harvested energy. Recently, therefore, research on solar-powered IoT (SP-IoT) has been actively pursued.

Solar-powered nodes (SP-nodes) can provide permanence in terms of energy by resolving the fundamental limitation of the energy capacity of the battery-based node; however, this does not imply the assurance of stable operation [5,6]. For example, there is the possibility that the amount of solar energy harvested by a node is not sufficient to operate the system normally due to external factors such as inclement weather or internal factors such as the inefficient operation of software. Among many issues within SP-IoT, therefore, research on the energy-adaptive behavior of SP-nodes has been extensively conducted.

These methods try to control the amount of consumed energy by configuring the duty cycle, sensing cycle, or data communication range. These efforts address performance degradation, but it should be noted that there are limits to the extent to which the performance can be compromised. Consequently, the node whose energy is continuously insufficient eventually enters a power outage state (sleep state) and thus cannot operate normally for a certain period. Since most IoT applications need stable operation as well as the persistent operation of nodes, a method to minimize the blackout time of nodes needs to be developed.

To solve this problem, a recent study used wireless power transfer (WPT) technology [7–9], which transmits radio frequency (RF) power wirelessly using an unmanned aerial vehicle (UAV) such as a drone. To efficiently supply the limited energy of a drone to the IoT field, the optimization scheme for charging mobility (which includes the movement path, charging location, and charging schedule) should be addressed. Our study addresses this optimization problem with a solution that is specifically tailored to the LoRaWAN-based SP-IoT environment. The proposed optimization method will henceforth be referred to as the max-min residual energy (MmRE) scheme. With our MmRE scheme, the drone transmits an appropriate amount of energy to all nodes that face a potential risk of future blackouts due to a lack of harvested energy, while making the best use of its limited energy. Consequently, the residual amount of energy of all IoT nodes becomes balanced, and more stable operation can be achieved. This contribution is summarized in Figure 1, and the distinctive features of this study can be summarized as follows.

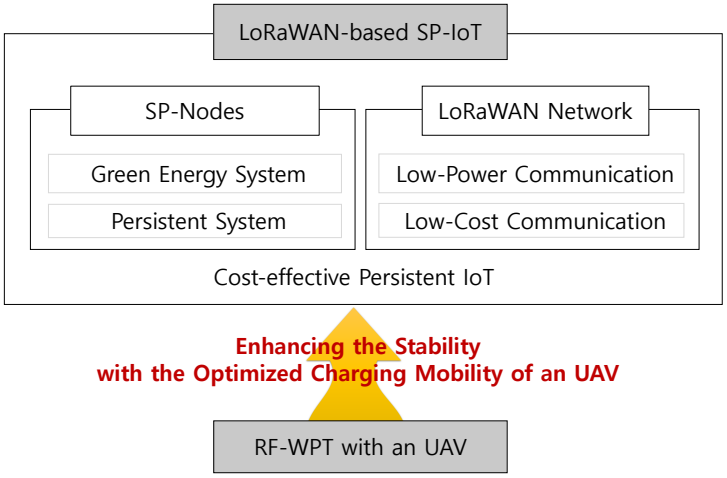

Figure 1. Contributions of the proposed scheme.

- **Considering the energy model for SP-nodes**: The proposed method establishes a threshold, based on existing research, to differentiate between nodes with insufficient energy and nodes with sufficient energy within the SP-nodes. Then, it transmits energy exclusively to nodes with insufficient energy, where the remaining energy falls below the threshold. Nodes with residual energy exceeding the threshold do not require WPT from the drone, as they operate normally with the currently harvested solar energy.
- **Considering the energy model of the drone**: The drone's energy is consumed for both flight and WPT. Therefore, even if the drone transmits energy only to nodes with insufficient energy, it may not be able to visit all of these nodes due to its limited energy.
- **Considering the characteristics of RF-WPT**: The RF-WPT technique enables the simultaneous charging of multiple nodes located around a single hovering location. Therefore, the method of transmitting energy by visiting every node for charging is inefficient.

This paper is organized as follows. Section 2 explains the latest relevant studies related to our research. Then, Section 3 describes the proposed MmRE scheme in detail and Section 4 verifies its performance through experiments. Finally, Section 5 presents the conclusions.

2. Related Work

2.1. Solar-Powered IoT

Battery-based IoT devices face operational challenges due to the limited amount of energy. In scenarios wherein a nodes depletes all the energy in a battery, it requires manual replacement or recharging. However, many IoT devices are deployed in natural environments that are inaccessible to humans, used for military tasks, ecological monitoring, and disaster detection, where maintenance is challenging. Maintenance in such environments increases the costs and complicates the large-scale deployment of these devices. To fundamentally address these energy constraint issues, research is underway to utilize rechargeable batteries that harvest environmental energy [10,11].

Energy harvesting involves converting environmental resources such as solar, geothermal, wind, hydro, and biomass energy into electrical energy. Solar energy, among the various sources, exhibits the highest energy density, as illustrated in Table 1. Furthermore, it follows a periodic pattern, allowing for the replenishment of new solar energy at harvesting intervals. Although not entirely precise, there is a certain degree of predictability in the supply. Considering these characteristics and accounting for the power consumption of typical IoT nodes, ranging from hundreds of watts to tens of watts, solar energy can be regarded as one of the most suitable and feasible energy sources for the continuous operation of IoT devices [12].

Table 1. Power density of energy harvesting [13].

Method	Power Density
Solar	6.63 W/m^2
Geothermal	2.24 W/m^2
Wind	1.84 W/m^2
Hydro	0.14 W/m^2
Biomass	0.08 W/m^2

SP-nodes are periodically recharged, allowing for continuity, but the fluctuation in the harvested energy introduces instability. Such instability can lead to degradation in the quality of service (QoS) for IoT applications or the quality of experience (QoE) for users. To prevent this, well-defined energy-harvesting models or energy usage models are essential. Kansal et al. [14] proposed an energy model and decision algorithm for solar-powered nodes to ensure continuous operation. Moser et al. [15] suggested a method using a moving average model to predict the collected energy quantity. Noh and Kang [16], as well as Zhang et al. [17], proposed time-agnostic balanced energy allocation techniques to reduce the significant fluctuations in the collected energy amount across different time intervals in a day. Moreover, Yang et al. [18] proposed an energy threshold value, enabling nodes to sustain their operation until the next cycle under any harvesting conditions. In our study, this energy threshold value is utilized.

2.2. Wireless Power Transmission for IoT

RF-WPT technology involves wirelessly transmitting electrical energy. Integrating WPT technology into a network proves to be an excellent solution to extend the lifespans of nodes by recharging batteries. In wireless IoT, charging devices are typically mounted on mobile wireless charging vehicles (WCVs) or UAVs to charge the IoT nodes wirelessly. Comparing WCVs, UAVs can reach IoT nodes more easily without using roads. Moreover, their high freedom of movement enables line of sight (LoS) measurement in short distances. Therefore, each device can be charged through this short-range LoS link from the UAV,

thus increasing the transmission efficiency of WPT without significant radio frequency losses [19,20].

Regarding WPT using UAVs, numerous studies have aimed to enhance the energy delivery efficiency by designing the charging path. Xu et al. [21] presented a UAV trajectory optimization mechanism to maximize the RF energy delivered to ground IoT devices based on the UAV's flight speed constraints. In this study, a continuous hover-and-fly trajectory was designed for the UAV to hover over a series of coordinates and fly in a straight line at maximum speed between each coordinate. Jiang et al. [22] addressed the joint optimization problem of the UAV path and time for wireless information and power transfer systems, which falls under the category of NP-hard problems. To tackle this complexity, they simplified the optimization process by making various assumptions. Recent studies [23,24] have analyzed one-dimensional and two-dimensional network trajectories of continuous hovering and flying. These studies propose solutions for the best use of WPT based on optimal trajectories.

While these studies can be applied to large-scale battery-based IoT, they face practicality challenges as they require UAVs with very large battery capacities to achieve long flight times and high WPT. However, our study is directed towards a LoRaWAN-based SP-IoT environment, where continuous operation is already viable from an energy standpoint. In this specific environment, our approach is designed to maximize stability of the IoT, based on the work of Xu et al. [21].

3. Proposed Method

This study introduces the max-min residual energy (MmRE) method to determine the optimal charging mobility of a drone. The MmRE scheme operates by predicting the residual energy of nodes that receive energy from the drone through WPT, aiming to maximize the smallest amount of remaining energy among them. Figure 2 provides an overview of the proposed method. Initially, as depicted in Figure 2a, the base station periodically gathers location and energy information, including the need for WPT charging and the current quantity of residual energy, from each node. Given the small size of this information, it can be piggybacked on RoLaWAN packets when each IoT device transmits sensory data to the base station. Therefore, the overhead resulting from this additional information transfer is negligible. Then, utilizing this information, the base station assesses the charging mobility of a drone for optimal WPT. Initially, it employs the MmRE method to choose hovering locations and determine the hovering time at each location. Subsequently, it calculates the path by which the drone can visit all hovering locations using the shortest path algorithm. Following this, as illustrated in Figure 2b, the drone moves to each hovering location along the path, simultaneously charging the nodes for the specified hovering time. By cyclically executing this process, the blackout time of the nodes is minimized, contributing to the stable and reliable operation of the nodes.

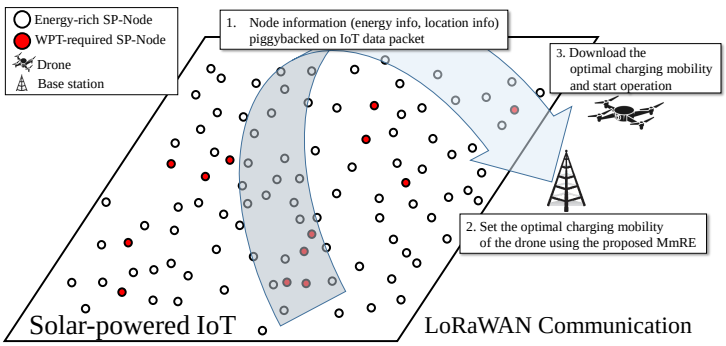

(**a**)

Figure 2. *Cont.*

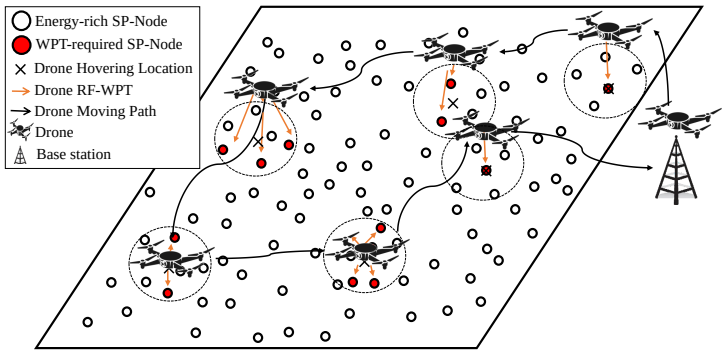

(**b**)

Figure 2. Operational overview of proposed MmRE scheme. (**a**) Operational sequence of MmRE scheme. (**b**) Example of drone's charging mobility obtained by MmRE scheme.

3.1. Energy Model

3.1.1. Energy Model of SP-Nodes

This section discusses the energy threshold for an SP-node to determine whether it requires energy from a drone. The energy threshold is associated with the energy-harvesting rate, the energy consumption rate, and the current residual energy of the node. The energy-harvesting rate is influenced by factors such as the solar panel type and size, location, weather, and season, while the energy consumption rate is affected by the data sensing rate, transmission range, and duty cycle. However, accurately predicting these factors is challenging. This study adopts a simple yet efficient energy model that does not require the precise prediction of these factors [12].

Let $P_{\text{solar}}(i)$ represent the average harvesting power of SP-node n_i, and let $P_{\text{sys}}(i)$ denote its average consumption power. The value of $P_{\text{sys}}(i)$ can be determined by continuously profiling the energy consumption during operation, while $P_{\text{solar}}(i)$ can be derived by profiling the harvested energy amount. Let the current available energy at node n_i be $E_{\text{residual}}(i)$; the expected time until the battery of node n_i is fully charged with $E_{\text{residual}}(i)$ can be expressed as follows:

$$T_{\text{full}}(E_{\text{residual}}(i)) = \frac{C(i) - E_{\text{residual}}(i)}{P_{\text{solar}}(i) - P_{\text{sys}}(i)}, \tag{1}$$

where $C(i)$ denotes the total battery capacity of the node. Note that the battery is charged only if the condition $P_{\text{solar}}(i) > P_{\text{sys}}(i)$ is satisfied. In this context, $P_{\text{solar}}(i)$ cannot be adjusted, but $P_{\text{sys}}(i)$ can be changed to the desired value by appropriately adjusting the system parameters, such as the duty cycle or transmission range of node n_i. Therefore, the condition $P_{\text{solar}}(i) > P_{\text{sys}}(i)$ can be satisfied by adjusting $P_{\text{sys}}(i)$.

In the meantime, accurately predicting the harvested energy amount is challenging due to the continuous variations in solar energy charge, influenced by the weather and time. However, a blackout will not occur from the current time until the battery is fully charged if the remaining energy in the battery meets the following condition:

$$E_{\text{residual}}(i) \geq P_{\text{sys}} \cdot T_{\text{full}}(E_{\text{residual}}(i)). \tag{2}$$

In other words, a node fulfilling (2) can function without experiencing a blackout until the subsequent battery is completely charged, even in adverse conditions. The application of (1) results in the derivation of (2) as follows:

$$E_{\text{residual}}(i) \geq \frac{P_{\text{sys}}(i)}{P_{\text{solar}}(i)} C(i). \tag{3}$$

To summarize, the system operates normally despite unforeseen circumstances, such as changes in weather or season, if the battery has an energy level greater than $\frac{P_{\text{sys}}(i)}{P_{\text{solar}}(i)}C(i)$. In this study, this condition is referred to as energy threshold $E_{\text{threshold}}(i)$ and is expressed as follows:

$$E_{\text{threshold}}(i) = \frac{P_{\text{sys}}(i)}{P_{\text{solar}}(i)}C(i). \tag{4}$$

Assuming that a node possesses residual energy $E_{\text{residual}}(i)$, which is less than $E_{\text{threshold}}(i)$, there is a risk of a blackout at node n_i. Consequently, this node requires an additional energy charge through WPT from the drone to ensure stable operation. Therefore, each node should transmit information regarding the need for WPT and the current residual energy amount, enabling the base station to calculate the optimal charging mobility.

3.1.2. RF-WPT Energy Model

To elucidate the RF-WPT energy model [21,25,26], we assume that each node n_i ($i \in I$) is stationary at the coordinate $(x_i, y_i, 0)$ on the ground, while the drone hovers at a fixed altitude H at time $t \in T$ before movement. Here, I represents the set of all nodes, and T is the total charging time. The changing location of the drone over time is denoted by $(x(t), y(t), H)$.

In this study, we employ the free space path loss model as the power transfer model for each node and the drone, assuming that most wireless channels between the drone and each node exhibit LoS. In this model, the channel power gain $h_i(t)$ between the drone and each node n_i at time t can be expressed as $\beta_0 d_i^{-2}(t)$. Here, β_0 denotes the channel power gain at the standard distance, and $d_i(t)$ represents the distance between node n_i and the drone at time t, denoted as $\sqrt{(x(t)-x_i)^2+(y(t)-y_i)^2+H^2}$. Assuming that the drone has a constant transmission power P_T, the RF power received by node n_i at time t can be defined as follows:

$$\begin{aligned} Q_i(x(t), y(t)) &= h_i(t)P_T \\ &= \frac{\beta_0 P_T}{(x(t)-x_i)^2+(y(t)-y_i)^2+H^2}. \end{aligned} \tag{5}$$

Utilizing Equation (5), the aggregate energy received by node n_i over the total charging time T can be formulated as follows:

$$\int_0^T Q_i(x(t), y(t))dt. \tag{6}$$

Finally, the remaining energy of node n_i after total charging time T is expressed as follows:

$$E_i(\{x(t), y(t)\}) = max\{C(i), \int_0^T Q_i(x(t), y(t))dt + E_{\text{residual}}(i)\}. \tag{7}$$

3.2. Problem Definition

As previously explained, the constrained energy capacity of the drone necessitates the optimal transmission of energy to nodes requiring charging. In this section, we provide a definition for the term 'the most efficient use'.

In addressing this optimization problem, we need to determine three factors: ① the hovering location, ② the hovering time at each location, and ③ the path required to visit all the hovering locations. To simplify the problem, we disregard the energy consumed by the drone during its flights between hovers, considering this negligible compared to the energy required for hovering and recharging. As a result, in our approach, ③ is determined using the shortest path algorithm in the final step. Consequently, our primary focus is on optimizing ① and ②. The critical parameter for the determination of ① and ② is the smallest value among the residual energy of the charged nodes after WPT completion. The objective function seeks to maximize this minimal energy amount. This function promotes

the equitable distribution of the drone's energy to nodes with insufficient energy, thereby enhancing the stability of the SP-IoT environment. The objective function can be expressed as follows:

$$\begin{aligned} &\max_{\{x(t),y(t)\}} \min_{k\in K} E_k(\{x(t), y(t)\}) \\ &s.t.\ K = \{i | E_{\text{residual}}(i) < E_{\text{threshold}}(i),\ i \in I\}. \end{aligned} \tag{8}$$

In summary, the problem addressed in this study involves finding the combination that satisfies the objective function (8) among the numerous combinations of hovering locations and hovering times. To tackle this problem, we employ the max-min residual energy (MmRE) method, which will be elucidated in the next subsection.

3.3. Max-Min Residual Energy (MmRE) Method

The proposed MmRE method aims to determine the hovering locations and the hovering time at each location. It is motivated by the work of Xu et al. [21] and is tailored to SP-IoT, approaching the problem by including not only the location information but also the energy information based on the SP-energy model. To this end, first, each node periodically transmits its WPT-related information to the base station, including its location, current energy, and the need for WPT charging. The need for for WPT charging is set when the current remaining energy is smaller than the threshold. Since we consider the LoRaWAN environment, the base station can receive the above data for each node by 1 hop from every node within a range of several kilometers; moreover, there is very little overhead because the data size is very small so they can be piggybacked on the IoT data packet.

After this, the base station finds the nodes that exhibit the need for WPT charging and adds them to the set of nodes to be charged by a drone in this WPT round. This set of nodes is denoted by K. The proposed MmRE method tries to solve the optimization problem regarding the objective function (7) for node n_k, $k \in K$, by applying Lagrange dual methods.

The objective function (8) can be redefined by introducing the auxiliary variable E as follows:

$$\begin{aligned} &\max_{\{x(t),y(t)\},E} E \\ &s.t.\ E_k(\{x(t), y(t)\}) \geq E,\ \forall k \in K. \end{aligned} \tag{9}$$

Equation (9) pertains to a non-convex optimization problem but adheres to the time-sharing condition [27]. Consequently, it can be treated as equivalent to its own Lagrange dual problem. Therefore, the problem expressed in (9) can be tackled utilizing the Lagrange dual method. If λ_k (which is not smaller than 0 for $\forall k \in K$) serves as a dual variable corresponding to the constraint in (9) for node n_k, then the associated Lagrangian for (9) is given by the following expression [28]:

$$\mathcal{L}(\{x(t), y(t)\}, E, \{\lambda_k\}) = (1 - \textstyle\sum_{k\in K} \lambda_k)E + \int_0^T \sum_{k\in K} \lambda_k Q_k(x(t), y(t))dt + \sum_{k\in K} \lambda_k E_{\text{residual}}(k). \tag{10}$$

Therefore, the dual function of the optimization problem of (9) is as follows:

$$f(\{\lambda_k\}) = \max_{\{x(t),y(t)\},E} L(\{x(t), y(t)\}, E, \{\lambda_k\}). \tag{11}$$

In order for (11) to uphold the upper limit (i.e., to satisfy $f(\{\lambda_k\}) < \infty$), it is essential to maintain the constraint $\sum_{k\in K} \lambda_k = 1$. With this condition incorporated, (11) can be formulated as follows:

$$\begin{aligned} &\min_{\lambda_k} f(\{\lambda_k\}) \\ &s.t.\ \sum_{k\in K} \lambda_k = 1,\ \lambda_k \geq 0,\ \forall k \in K. \end{aligned} \tag{12}$$

Finally, the optimization problem (9) can be solved by addressing (12), which represents its dual problem. The set of feasible values for $\{\lambda_k\}$ that adhere to the constraint in (12) is denoted as X. Initially, solving (11) yields $f(\{\lambda_k\})$ for a given set of feasible dual variables $\{\lambda_k\} \in X$. Subsequently, (12) is solved to identify the optimal $\{\lambda_k\}$ that minimizes $f(\{\lambda_k\})$. The optimal dual solution to (12) is denoted as $\{\lambda_k^*\}$. Finally, the primal solution of (9), representing the original problem, must be determined based on $\{\lambda_k^*\}$. The primal solutions corresponding to the optimal dual solution $\{\lambda_k^*\}$ are expressed as $(\{x^*(t)\}, \{y^*(t)\}, E^*)$.

Note that when utilizing the Lagrange dual method to solve problem (8) through the dual problem (12), the optimal solution for problem (11) under the optimal dual solution $\{\lambda_k^*\}$ serves as the optimal primal solution for problem (8), provided that such a solution is unique. Conversely, if the optimal solution $\{\lambda_k^*\}$ for problem (11) is non-unique, it may not be both feasible and optimal for problem (8) in general. Consequently, an additional step involving time sharing among these non-unique optimal solutions is necessary to obtain the optimal primal solution for $\{x^*(t)\}$, $\{y^*(t)\}$ and E^* in problem (8).

Under the optimal dual solution $\{\lambda_k^*\}$, optimal location solutions, which are denoted by $(x_1^*, y_1^*), ..., (x_\Gamma^*, y_\Gamma^*)$, where Γ is the total number of hovering locations, are obtained via an exhaustive search for the 2D arrangement area of IoT nodes. If the computing power is constrained or there is a need to save time, heuristic search or sub-optimal search techniques [29] can be employed. Due to the zero duality gap between (9) and (12), it is evident that, for any time $t \in [0, T]$, the optimal primal solution of $(x^*(t), y^*(t))$ must be chosen from the Γ hovering locations.

Once the hovering locations are determined, we must determine the amount of time for which the drone should hover and charge the nodes at each hovering location. Let us denote the total time for the drone to start charging and return as T. Note that when the drone hovers at the same location at different times t, the nodes will receive the same amount of power. Therefore, we only need to determine the time-sharing ratio among the Γ solutions to construct the optimal primal solution to (9). Here, time sharing means that the drone should hover at each of these different locations for a certain portion of the total duration T. Let τ_γ^* denote the optimal hovering time at each hovering location $(x_\gamma^*, y_\gamma^*, H)$, where γ is an integer that satisfies $\gamma \in [1, \Gamma]$. Then, τ_γ^*, together with the maximum min-energy E^*, can be obtained by solving the following equation:

$$\begin{aligned} &\max E \\ &\text{s.t.} \sum_{\gamma=1}^{\Gamma} \tau_\gamma Q_k(x_\gamma^*, y_\gamma^*, H) + E_{\text{residual}}(k) \geq E, \forall k \in K \\ &\sum_{\gamma=1}^{\Gamma} = T. \end{aligned} \tag{13}$$

This problem can be solved using a general convex optimization technique [28] because it is a linear programming (LP) problem.

When the hovering location $(x_\gamma^*, y_\gamma^*, H)$ and the hovering time for each location τ_γ^* are determined, finally, the sequence by which the drone will visit these locations must be determined. As explained before, our approach does not take into account the energy consumed by the drone for its flights between hovers, because it is negligible compared to the energy required for hovering and recharging. Therefore, a simple shortest path algorithm is employed to determine the path.

4. Experimental Results

To conduct the performance evaluation of the proposed scheme, we modified and utilized SolarCastalia [30], a solar-energy-harvesting IoT simulator. As performance metrics, we measured the number of nodes experiencing power outages during the experimental period and the amount of sensing data transmitted to the base station.

4.1. Experimental Environments

A simulation experiment was conducted to validate the performance of the proposed method. The comparative methods targeted for the performance evaluation were as follows: ① a technique operating solely with solar energy, without WPT (NoWPT); ② a technique involving visits to all nodes requiring WPT, performing WPT for an equal duration (SameWPT); and finally, ③ a technique applying MmRE to all nodes without considering the solar energy model and irrespective of the energy threshold values [21] (BatteryMmRE).

For the experimental setup, the field area of the IoT nodes was fixed at 1 km × 1 km, and 10,000 nodes were randomly deployed. The experiment comprised a total of 10,080 simulation rounds, with each round representing one hour. The WPT charging cycle for the drones was set to once a day, and the drone's battery capacity for WPT was 15,000 mAh. The flight time of the drone, including hovering, was within one hour, and a separate 10,000 mAh battery was assumed to be available for this purpose. Each node, utilizing LoRaWAN, transmitted sensing data to a base station located within 2 km. The solar energy harvested for each node was determined by randomly selecting weather conditions in SolarCastalia, simulating energy collection over time. The daily harvested energy ranged between 15 J/day and 25 J/day as a random value. To ensure the persistent operation of the nodes, the consumption energy did not exceed the collected energy based on the harvest cycle, commonly referred to as energy-neutral operation (ENO). The SP-IoT devices were configured to perform ENO by default, setting the consumption energy to a random value between 15 J/day and 25 J/day, similar to the harvested amount. It is important to note that despite aligning the energy consumption as much as possible with ENO, there exists a minimum energy requirement for the basic operation of the device. If the continuously decreasing collected energy does not satisfy this minimum energy requirement, the remaining energy may fall below the threshold, causing the node to enter a temporary blackout state. The key experimental parameters are presented in Table 2.

Table 2. Major experimental parameters.

Parameter	Value
Simulation time	10,080 ticks
Period of drone's charging	1 h
Field size	1 km × 1 km
Number of nodes	10,000
Sensor node battery capacity	150 mAh
Sensing data transfer rate	1 kB/min
LoRa data transmission range	2 km
Amount of harvested energy	15–25 J/day
Amount of consumed energy	15–25 J/day
Duty cycle	0.5
Battery capacity of drone for WPT	15,000 mAh
Hovering height of drone (H in Equation (5))	5 m
Total hovering time (T in Equation (13))	1 h

4.2. Number of Nodes Experiencing a Blackout

Figure 3 depicts a graph showing the cumulative count of blackout nodes for each scheme after conducting experiments in the basic experimental environment outlined in Table 2. In other words, it represents the total number of instances of blackouts during the experimental period. Note that, even if a blackout occurs, normal operation resumes once the WPT or solar energy is replenished. The NoWPT mode, being a scheme without additional energy transfer, exhibits the highest number of blackout nodes compared to other schemes. The SameWPT mode, due to the limited energy of the drone, results in many nodes experiencing blackouts as it performs the same amount of WPT for each node, regardless of each node's residual energy. BatteryMmRE, attempting WPT for all nodes without considering the energy threshold values of the solar energy model, tries to

maximize the smallest residual energy value after charging among them. However, due to the constrained energy of the drone, it cannot transmit sufficient energy to nodes in dire need of WPT, resulting in a higher number of blackout nodes compared to the proposed scheme. In the proposed scheme, selecting nodes in need of WPT and performing MmRE on only those nodes efficiently utilizes the drone's limited energy, leading to a significant reduction in the number of blackout instances. This signifies enhanced stability in IoT.

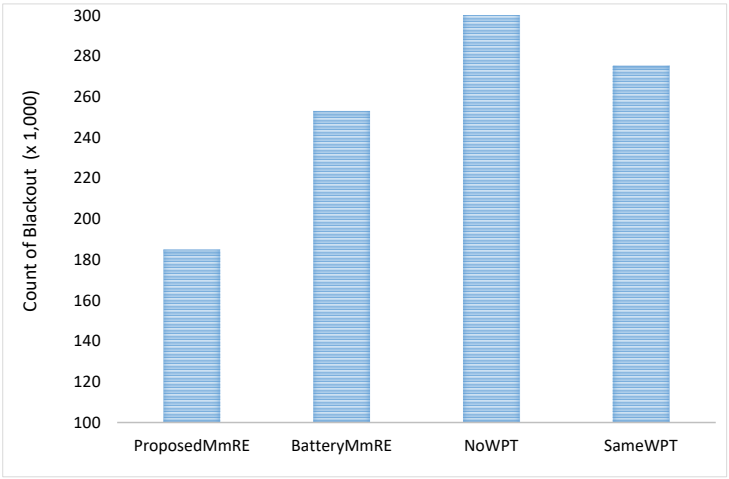

Figure 3. Cumulative count of blackout nodes for each scheme.

4.3. Amount of Data Collected at the Base Station

Figure 4 represents a graph indicating the total amount of data collected by the base station for each mode after 10,080 rounds in the given simulation environment. While we previously examined the number of blackout instances, the data collection amount reflects not only the frequency of blackouts but also the amount of time for which the node remains in the blackout state. Therefore, the data collection amount tends to be smaller when there are more blackout nodes and the blackout duration is longer. Although the data collection amount shows a similar trend to the frequency of occurrence of blackout nodes, the differences between the schemes become more pronounced. This indicates that the efficient execution of WPT affects not only the frequency of blackouts but also the blackout duration. Focusing on performing WPT intensively on blackout nodes to quickly restore normal operation is crucial. However, other schemes are unable to do so, leading to a longer blackout duration and ultimately reducing the amount of collected data dramatically.

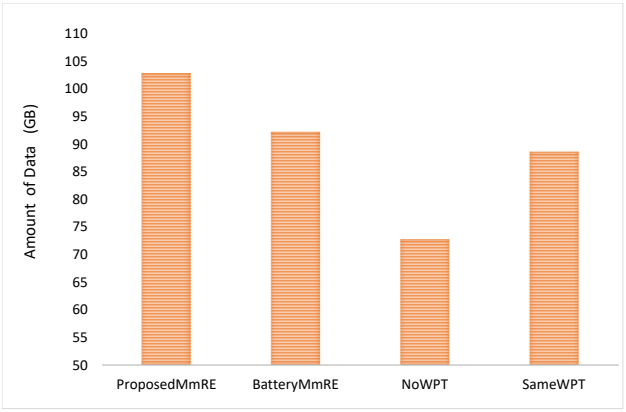

Figure 4. Cumulative amount of collected data for each scheme.

4.4. Performance Comparison Based on Field Size

Figure 5a,b depict the number of blackout nodes and data collection amount based on the field size. The field size of 1 corresponds to the default field size described in

Table 2, while 0.1 and 0.01 represent sizes at a 1/10 and 1/100 ratio of the default field size, respectively. Overall, it is observed that the performance of almost all schemes improves with smaller field sizes. This is because smaller field sizes result in higher node densities, leading to the increased efficiency of WPT. In other words, in a smaller field, it signifies that one WPT attempt at a given location enables charging for a greater number of nearby nodes.

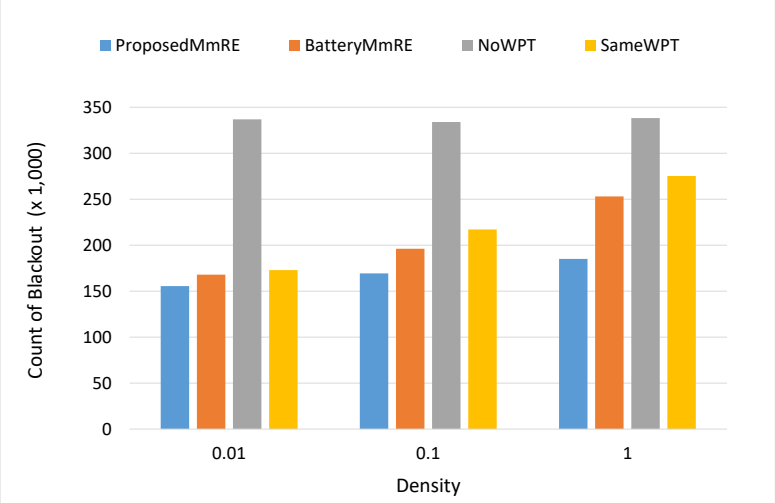

(**a**)

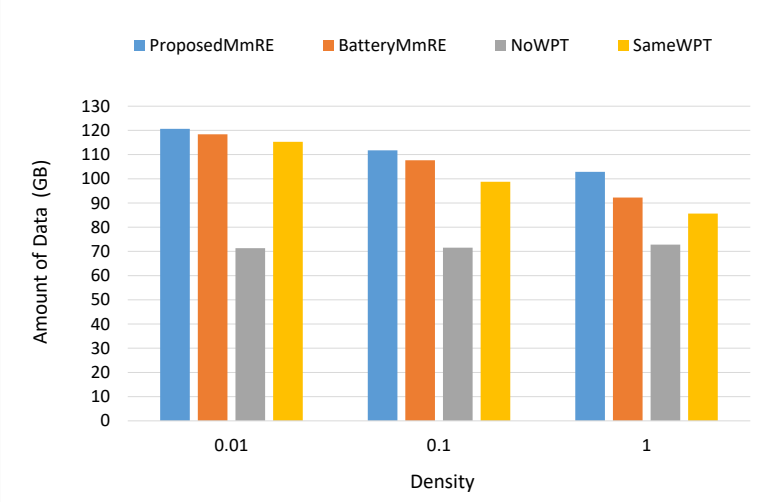

(**b**)

Figure 5. Blackout nodes and data collection amounts based on field size. (**a**) Cumulative count of blackout nodes. (**b**) Cumulative amount of collected data.

Note that as the field size increases, the performance difference between the proposed scheme and other schemes becomes more pronounced. This is attributed to the reduced significance of the optimal charging locations and charging time selection when the node density is high. This means that where and for how long the drone performs WPT is less important in higher-density environments because a greater number of nodes can be charged for each WPT round. Therefore, it can be said that the proposed scheme is more beneficial in areas with relatively lower node densities.

4.5. Performance Comparison Based on the Number of Nodes

Figure 6a,b depict the number of blackout nodes and data collection amount when the number of nodes (1000, 2000, 3000) is increased while maintaining the same node density. As evident in the figures, due to the absolute difference in the number of nodes, the values

of each performance metric are proportionate to the number of nodes. However, it is crucial to note that as the number of nodes increases, the performance difference between the proposed scheme and other schemes becomes more pronounced. This is because, with a higher number of nodes, the optimization related to the selection of target nodes for WPT and mobility decisions becomes more critical due to the constrained energy of the drone.

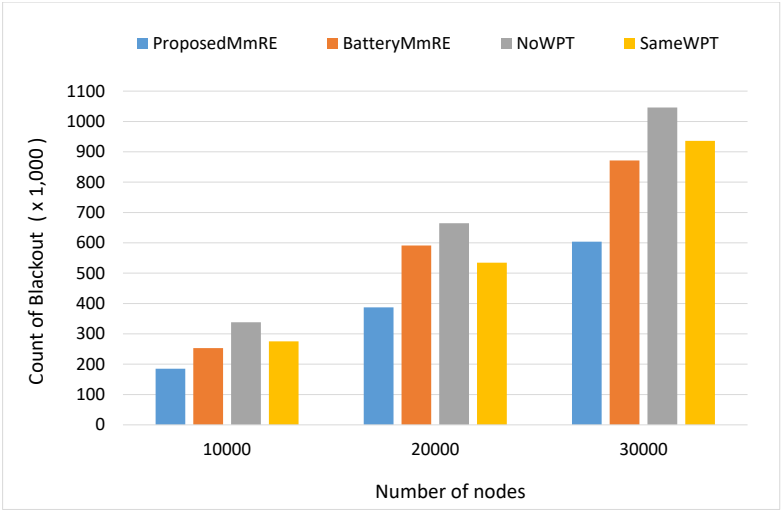

(**a**)

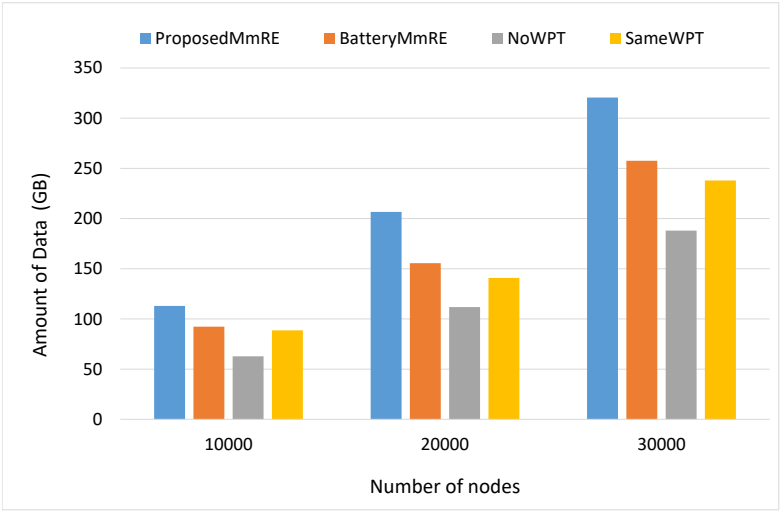

(**b**)

Figure 6. Blackout nodes and data collection amount based on number of nodes. (**a**) Cumulative count of blackout nodes. (**b**) Cumulative amount of collected data.

4.6. Comparison Based on Drone's Battery Capacity

Figure 7 illustrates the performance of each scheme as the drone's battery capacity varies. Generally, as the drone's battery capacity increases, the utility of WPT improves, resulting in enhanced performance for most schemes, excluding the NoWPT scheme. It is noteworthy that the performance gap between the proposed scheme and other schemes becomes more pronounced as the drone's battery capacity decreases. This demonstrates that the proposed scheme is the most efficient in utilizing the drone's limited energy resources, meaning that a high level of stability can be achieved even with a drone having a small battery capacity.

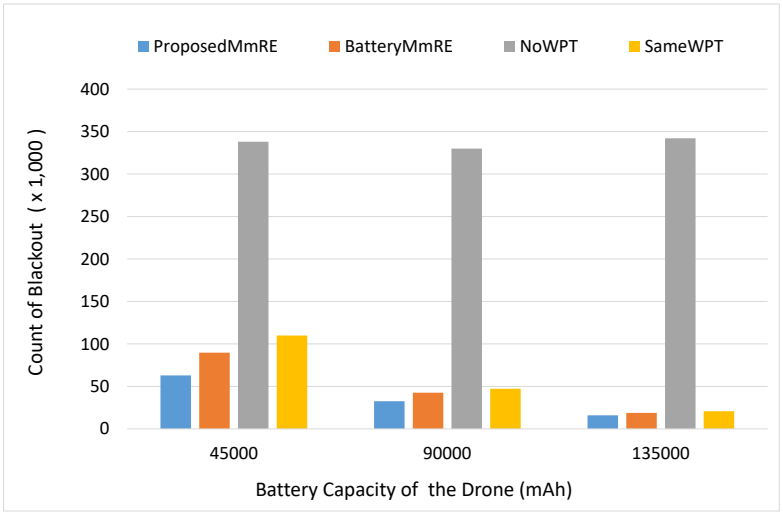

(**a**)

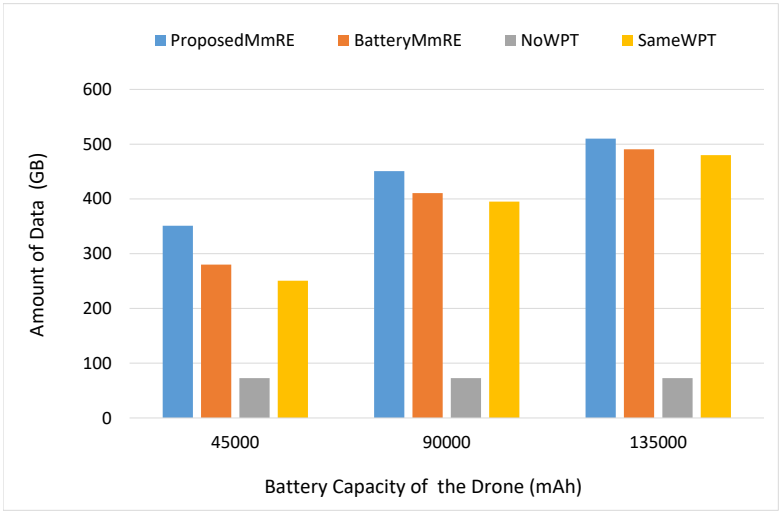

(**b**)

Figure 7. Blackout nodes and data collection amount based on the battery size. (**a**) Cumulative count of blackout nodes. (**b**) Cumulative amount of collected data.

4.7. Example of Drone's Energy Level Variations

Figure 8 illustrates an example of the drone's remaining energy levels during its movement while performing WPT using the proposed MmRE. As mentioned earlier, the maximum duration for movement, including hovering, in this experiment is 1 h, and the initial energy capacity for WPT is 15,000 mAh. In this particular example, the optimization results in hovering at a total of 10 spots, and the drone hovers at each spot during the hovering time shown in Figure 8, performing WPT in the airspace at a height of 5 m. Therefore, with each passage through a spot, a decrease in the remaining energy level can be observed. It is noticeable that the hovering time at spot 4 is the longest, indicating that a significant amount of energy was utilized for WPT during this period. Consequently, there is a substantial decrease in the remaining energy when moving to the next spot, spot 5. Upon visiting the final spot, spot 10, it can be observed that all remaining energy is used for WPT, indicating that our scheme maximizes the utilization of the drone's energy.

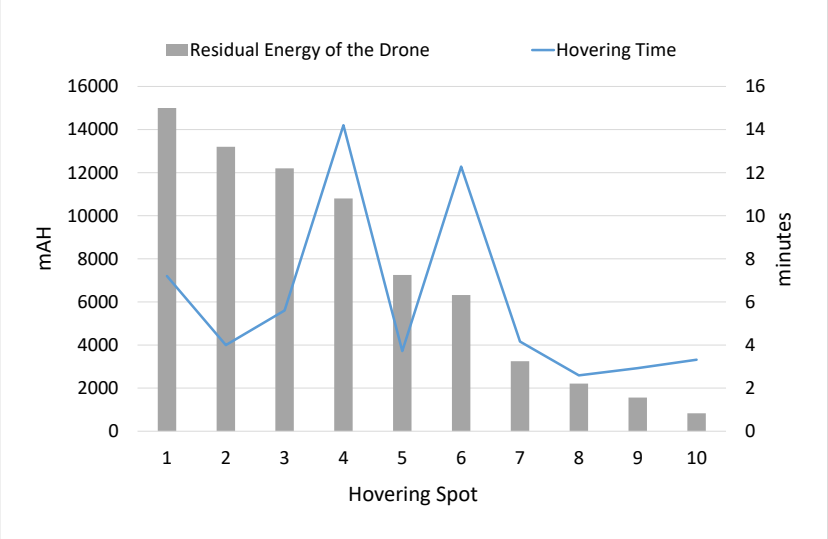

Figure 8. WPT duration at each hovering spot and the variation in the drone's energy level.

4.8. Analysis of Time Complexity

The computational complexity of optimization problems of the min-max or max-min form is naturally characterized by π_2^P, the second level of the polynomial-time hierarchy. However, the proposed method transforms the given optimization primal problem into a convex optimization problem using the Lagrangian dual function. The interior point method, a representative algorithm for convex optimization, requires time complexity of $O(n^{3.5}log(1/\varepsilon))$ to achieve precision of ε when there are n variables and m constraints (for the case in which $n \geq m$). Since BatteryMmRE fundamentally employs the same optimization scheme, it necessitates similar time complexity. On the other hand, SameWPT and NoWPT have time complexity of $O(1)$. However, this optimization is performed once per WPT cycle at a resource-rich base station, mitigating concerns about the overall time complexity.

5. Conclusions

Solar energy contributes to the sustainability of IoT from an energy perspective. However, this does not imply that solar energy can guarantee the stable operation of IoT nodes. This is the reason for which WPT was adopted in this study. Considering that WPT can enhance the stability of SP-nodes, this study proposed the MmRE scheme, which is a charging mobility determination scheme for drones for efficient energy charging to maximize the stability in a LoRaWAN-based SP-IoT environment.

With the proposed MmRE scheme, the drone determines ① the hovering location for charging, ② the hovering time (charging time) at each location, and ③ a path that visits all hovering locations. The objective function in the MmRE scheme aims to maximize the quantity of the smallest residual energy among all nodes. This objective function enables the drone to distribute its energy to the nodes with insufficient energy in a well-balanced manner, thereby enhancing the stability of the SP-IoT environment. The experimental results indicate that the MmRE scheme significantly reduces the blackout times for each node by more than half compared to existing methods. Consequently, this scheme could increase the amount of data collected at the LoRaWAN base station by over 15%. Furthermore, it was observed that MmRE showed even stronger performance in environments with a higher node density in IoT scenarios.

The proposed method is expected to contribute to developing a sustainable or green IoT and also expanding the markets in this field by securing operational stability in SP-IoT applications.

Author Contributions: Conceptualization, D.K.N. and Y.G.; methodology, I.Y.; software, Y.G.; validation, I.Y. and Y.G.; formal analysis, D.K.N.; writing—original draft preparation, D.K.N.; project administration, I.Y.; funding acquisition, D.K.N. All authors have read and agreed to the published version of the manuscript.

Funding: This work was supported by a National Research Foundation of Korea (NRF) grant funded by the Korean government (MEST) (2021R1A2C1005919).

Data Availability Statement: The original contributions presented in the study are included in the article, further inquiries can be directed to the corresponding author.

Conflicts of Interest: The authors declare no conflicts of interest.

References

1. Augustin, A.; Yi, J.; Clausen, T.; Townsley, W.M. A study of LoRa: Long range & low power networks for the internet of things. *Sensors* **2016**, *16*, 1466–2016. [CrossRef] [PubMed]
2. Eigner, H. Interference Analysis of LoRaWAN Systems. Ph.D. Thesis, TU Wien, Vienna, Austria, 2021.
3. Sudevalayam, S.; Purushottam, K. Energy harvesting sensor nodes: Survey and implications. *IEEE Commun. Surv. Tutor.* **2010**, *13*, 443–461. [CrossRef]
4. Sah, D.K.; Amgoth, T. Renewable energy harvesting schemes in wireless sensor networks: A survey. *Inf. Fusion* **2020**, *63*, 223–247. [CrossRef]
5. Kanoun, O.; Bradai, S.; Khriji, S.; Bouattour, G.; El Houssaini, D.; Ben Ammar, M.; Naifar, S.; Bouhamed, A.; Derbel, F.; Viehweger, C. Energy-Aware System Design for Autonomous Wireless Sensor Nodes: A Comprehensive Review. *Sensors* **2021**, *21*, 548. [CrossRef] [PubMed]
6. Cinco-Solis, A.; Camacho-Escoto, J.J.; Orozco-Barbosa, L.; Gomez, J. PPAASS: Practical Power-Aware Duty Cycle Algorithm for Solar Energy Harvesting Sensors. *IEEE Access* **2022**, *10*, 117855–117870. [CrossRef]
7. Vilathgamuwa, D.M.; Sampath, J.P.K. Wireless power transfer (WPT) for electric vehicles (EVS)—Present and future trends. In *Plug in Electric Vehicles in Smart Grids*; Springer: Singapore, 2015; pp. 33–60.
8. Xie, L.; Shi, Y.; Hou, Y.T.; Lou, A. Wireless power transfer and applications to sensor networks. *IEEE Wirel. Commun.* **2013**, *20*, 140–145.
9. Chen, J.; Chang, W.Y.; Ouyang, W. Efficient wireless charging pad deployment in wireless rechargeable sensor networks. *IEEE Access* **2020**, *8*, 39056–39077. [CrossRef]
10. Yuksel, M.E.; Fidan, H. Energy-aware system design for batteryless LPWAN devices in IoT applications. *Ad Hoc Netw.* **2021**, *122*, 102625. [CrossRef]
11. Giuliano, F.; Pagano, A.; Croce, D.; Vitale, G.; Tinnirello, I. Adaptive algorithms for batteryless lora-based sensors. *Sensors* **2023**, *23*, 6568. [CrossRef]
12. Cheong, S.H.; Kang, M.; Kim, Y.; Park, M.; Park, J.; Noh, D.K. Solar-CTP: An Enhanced CTP for Solar-Powered Wireless Sensor Networks. *IEEE Access* **2020**, *8*, 127142–127155. [CrossRef]
13. Zalk, J.V.; Behrens, P. The spatial extent of renewable and non-renewable power generation: A review and meta-analysis of power densities and their application in the U.S. *Energy Policy* **2018**, *123*, 83–91. [CrossRef]
14. Kansal, A.; Potter, D.; Srivastava, M.B. Performance aware tasking forenvironmentally powered sensor networks. In Proceedings of the Joint International Conference on Measurement and Modeling of Computer Systems, New York, NY, USA, 10–14 June 2004; pp. 223–234.
15. Moser, C.; Thiele, L.; Brunelli, D.; Benini, L. Adaptive power management in energy harvesting systems. In Proceedings of the Design, Automation and Test in Europe Conference and Exhibition, Nice, France, 16–20 April 2007; pp. 1–6.
16. Noh, D.K.; Kang, K. Balanced energy allocation scheme for a solar-powered sensor system and its effects on network-wide performance. *J. Comput. Syst. Sci.* **2011**, *77*, 917–932. [CrossRef]
17. Zhang, Y.; He, S.; Chen, J. Data gathering optimization by dynamic sensing and routing in rechargeable sensor networks. *IEEE/ACM Trans. Netw.* **2016**, *24*, 1632–1646. [CrossRef]
18. Yang, Y.; Wang, L.; Noh, D.K.; Le, H.K.; Abdelzaher, T.F. SolarStore: Enhancing data reliability in solar-powered storage-centric sensor networks. In Proceedings of the 7th International Conference on Mobile Systems, Applications, and Services, Kraków, Poland, 22–25 June 2009; pp. 333–346.
19. Hu, Y.; Yuan, X.; Zhang, G.; Schmeink, A. Sustainable Wireless Sensor Networks with UAV-Enabled Wireless Power Transfer. *IEEE Trans. Veh. Technol.* **2021**, *70*, 8050–8064. [CrossRef]
20. Baek, J.; Han, S.I.; Han, Y. Optimal UAV route in wireless charging sensor networks. *IEEE Internet Things J.* **2019**, *7*, 1327–1335. [CrossRef]
21. Xu, J.; Zeng, Y.; Zhang, R. UAV-enabled wireless power transfer: Trajectory design and energy optimization. *IEEE Trans. Wirel. Commun.* **2018**, *17*, 5092–5106. [CrossRef]
22. Jiang, M.; Li, Y.; Zhang, Q.; Qin, J. Joint position and time allocation optimization of UAV enabled wireless powered communication networks. *IEEE Trans. Commun.* **2019**, *67*, 3806–3816. [CrossRef]

23. Hu, Y.; Yuan, X.; Xu, J.; Schmeink, A. Optimal 1D trajectory design for UAV-Enabled multiuser wireless power transfer. *IEEE Trans. Commun.* **2019**, *67*, 5674–5688. [CrossRef]
24. Yuan, X.; Yang, T.; Hu, Y.; Xu, J.; Schemink, A. UAV trajectory design for UAV-Enabled multiuser nonlinear wireless power transfer. *IEEE Trans. Wirel. Commun.* **2021**, *20*, 1105–1121. [CrossRef]
25. Guo, S.; Wang, F.; Yang, Y.; Xiao, B. Energy-efficient cooperative for simultaneous wireless information and power transfer in clustered wireless sensor networks. *IEEE Trans. Commun.* **2015**, *63*, 4405–4417. [CrossRef]
26. Sansoy, M.; Buttar, A.S.; Goyal, R. Empowering wireless sensor networks with rf energy harvesting. In Proceedings of the 7th International Conference on Signal Processing and Integrated Networks (SPIN 2020), Noida, India, 27–28 February 2020; pp. 273–277.
27. Kotary, J.; Fioretto, F.; van Hentenryck, P.; Wilder, B. End-to-end constrained optimization learning: A survey. *arXiv* **2021**, arXiv:2103.16378.
28. Boyd, S.; Boyd, S.P.; Vandenberghe, L. *Convex Optimization*; Cambridge University Press: Cambridge, UK, 2004; ISBN 0-521-83378-7.
29. Stern, R.; Kiesel, S.; Puzis, R.; Felner, A.; Ruml, W. Max is more than min: Solving maximization problems with heuristic search. In Proceedings of the 2014 International Symposium on Combinatorial Search, Prague, Czech Republic, 15–17 August 2014; Volume 5, pp. 148–156.
30. Yi, J.M.; Kang, M.J.; Noh, D.K. SolarCastalia: Solar energy harvesting wireless sensor network simulator. *Int. J. Distrib. Sens. Netw.* **2015**, *11*, 415174. [CrossRef]